INTERNAL WAVE GENERATION BY A TURBULENT BOTTOM BOUNDARY LAYER

JOHN R. TAYLOR, SUTANU SARKAR

Mechanical and Aerospace Engineering, University of California, San Diego
9500 Gilman Dr. La Jolla, CA 92093-0411

Abstract. Internal gravity waves excited by the turbulent motions in a bottom Ekman layer are examined using large eddy simulation. The outer flow is steady and uniformly stratified while the density gradient is set to zero at the flat lower wall. After initializing with a linear density profile, a mixed layer forms near the wall separated from the ambient stratification by a pycnocline. Internal waves are observed radiating away from the boundary layer with a group velocity primarily directed $35-60^o$ from the vertical axis, consistent with previous laboratory studies. A viscous internal wave model is invoked to explain the observed frequency spectrum of the vertically propagating waves. The energy flux associated with the radiated waves is found to be small compared to the integrated dissipation in the boundary layer, but is of the same order as the integrated buoyancy flux.

1. Introduction

When turbulence is present in a stably stratified fluid, internal gravity waves are often created and radiate energy away from the source region. Turbulence-generated internal waves have been observed in a variety of flows: wakes [3, 9, 11, 4], shear layers [13, 12, 2], in the lee of topography [1], grid-generated turbulence [10, 7, 5, 6] and gravity currents [8]. The turbulence that generates the internal waves may be associated with an essentially well-mixed region (e.g. grid turbulence) or a stratified region (e.g. wakes and shear layers). This study will be focused on an example of the former case. Turbulence-generated internal waves may be important to the flow evolution since they are capable of extracting energy and momentum from a forced region, propagating to another nearby or remote location, and depositing their energy and momentum through a variety of possible mechanisms (e.g. wave breaking, wave/wave interactions, critical layer absorption)

The importance of turbulence-generated internal waves to the growth of a mixed region was considered by Linden [10]. An oscillating grid was used to generate a turbulent mixed layer above a density stratified region. As the mixed layer deepened, a pycnocline developed with a density gradient up to three times the value in the outer region. Internal waves were observed propagating away from the mixed region when the outer layer had a linear stratification instead of being homogeneous. The relative importance of the internal waves was quantified by comparing the rate of change of potential energy to the internal wave energy flux, and it was found that the presence of propagating internal waves may reduce the mixed layer growth by up to 50%. A different conclusion was reached by E and Hopfinger [7] who also considered shear-free grid generated turbulence. With two initial conditions, a uniformly stratified fluid and a two-layer system, they found that the rate of mixed layer growth depends on the density jump at the interface, but not on the density structure away from the mixed region. Based on this observation, and an estimate of the internal wave energy flux relative to the turbulence flux, they concluded that radiated internal waves, which exist only in the continuously stratified case, do not significantly affect the growth of the mixed layer.

Sutherland and Linden [13] conducted a laboratory experiment with stratified fluid flowing over a vertical barrier. A turbulent shear layer formed in the wake of the barrier and internal waves were observed propagating away from the shear layer through the uniformly stratified surrounding fluid. The largest amplitude waves were associated with an angle of propagation in the range $45^o < \Theta < 60^o$. Dohan and Sutherland [5] described laboratory experiments using an oscillating grid to create a turbulent mixed region in a uniformly stratified tank. A novel visualization technique was used in order to examine the internal waves in detail. The background buoyancy frequency was varied by over a factor of 4 and in all cases the frequency of the waves was such that the vertical angle of propagation was between $42^o < \Theta < 55^o$.

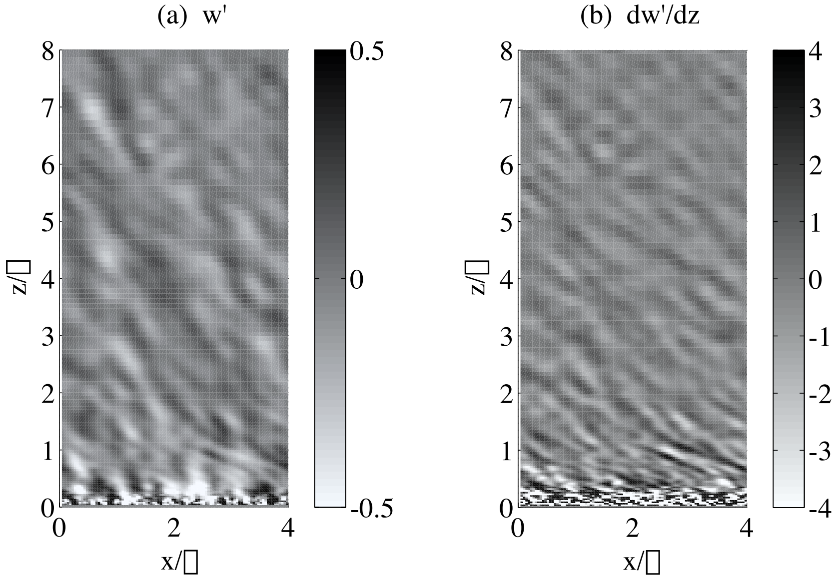

Figure 1. Instantaneous vertical velocity for the case with $Ri_* = 1000$ at $tf = 20$. At this time, the maximum temperature gradient in the pycnocline occurs at about 0.275 δ.

Since the turbulent region that provides energy to the wave field is composed of many spatial and temporal scales, it is perhaps surprising that the turbulence-generated internal waves are often associated with a relatively narrow frequency band that is proportional to the local buoyancy frequency. The angle made by the group velocity vector and the vertical direction is set from the dispersion relation, which for non-rotating, linear internal gravity waves is $\omega = N cos\, \Theta$, where ω is the intrinsic frequency, N is the background buoyancy (or Brunt-Väisälä) frequency, and Θ is the angle made between the wavenumber vector and the horizontal axis. Therefore, waves with a particular frequency are also associated with a characteristic angle of propagation. Previous studies of turbulence-generated internal waves have generally found that $35^o < \Theta < 60^o$.

The present study is based on simulations of a bottom Ekman layer with a uniform density stratification outside the boundary layer. The focus of this paper will be on the internal waves excited by turbulent motions in the bottom boundary layer. While previous laboratory and 2-D numerical studies have considered the generation of internal waves from a well-mixed turbulent region, this has not yet been examined in the case of boundary layers. The three-dimensional structure of the waves will be examined, and compared with the general characteristics of turbulence-generated internal waves previously observed in laboratory experiments. The importance of the radiated internal waves to the dynamics of the boundary layer will also be addressed by comparing the internal wave energy flux to the integrated turbulent dissipation rate and the integrated buoyancy flux.

2. Formulation

The turbulent boundary layer that is considered here is generated when a steady flow in geostrophic balance encounters a smooth, flat wall. Near the wall, where the turbulent viscosity contributes to the leading order momentum balance, the flow turns in the direction of the pressure gradient, forming the well-known Ekman spiral. A constant density gradient is applied as the upper boundary condition while the density gradient is set to zero at the wall. Since a large eddy simulation is used to examine this flow, the filtered governing equations are numerically integrated in time. Using the friction velocity, u_*, the turbulent Ekman layer depth, $\delta = u_*/f$, and the outer layer density gradient, $d\rho/dz_\infty$, the following nondimensional parameters can be formed:

$$Re_* = \frac{u_* \delta}{\nu}, \quad Ri_* = -\frac{g}{\rho_0}\frac{d\rho}{dz}_\infty \frac{\delta^2}{u_*^2} = \frac{N_\infty^2}{f^2}, \quad Pr = \frac{\nu}{\kappa}. \tag{1}$$

Here, ρ_0 is the constant density which has been used to apply the Boussinesq approximation, ν is the molecular kinematic viscosity, κ is the molecular diffusivity, f is the Coriolis parameter, and N_∞ is the free stream buoyancy frequency. Density changes are assumed to be caused by temperature variation in water, motivating the choice of Prandtl number, $Pr = 5$. We have performed simulations at three different values of Ri_*, namely 0, 100, and 1000. Changing Ri_* is equivalent to changing the free-stream temperature gradient, except when $Ri_* = 0$ and the temperature acts like a passive scalar. The friction Reynolds number is $Re_* = 960$. The flow is simulated with a near-wall model large eddy simulation (NWM-LES) using a dynamic mixed model, see Taylor and Sarkar [14] for details.

3. Observations of turbulence-generated internal waves

The internal wave field generated by the boundary layer at quasi-steady state is shown through instantaneous x-z slices of w' and $\partial w'/\partial z$ in Figure 1. We have found that the vertical velocity field contains a significant non-propagating component in the outer layer and that $\partial w'/\partial z$ more clearly shows the phase lines of the propagating waves which slant up and to the left. For internal waves, the group velocity, $\mathbf{c}_g$, is perpendicular to the wavenumber vector and parallel to the phase lines. Note that the direction of the phase lines is the same as would be seen for topographically generated waves with a flow in the positive x-direction. It is visually evident from Figure 1(b) that just above the pycnocline, for $0.5 < z/\delta < 1.5$, there are internal waves with phase lines forming a larger angle with the vertical direction compared to the waves in the outer layer. Since the dispersion relation for linear internal waves under the presence of rotation is $\omega^2 = N^2 cos^2\Theta + f^2 sin^2\Theta$, and $f^2 << N^2$, this implies that low frequency waves exist just above the pycnocline that are not observed far from the boundary layer.

The turbulence-generated internal waves in the simulations exhibit a characteristic propagation angle in the horizontal and vertical directions. This is illustrated for $Ri_* = 100$ and $Ri_* = 1000$ in Figure 2. Part (a) shows the horizontal wavenumbers corresponding to the maximum amplitude of $\partial w'/\partial z$, and part (b) shows the corresponding azimuthal angle, ϕ made by the wavenumber vector, formed by the components in part (a), and the x-axis. The dominant streamwise wavenumber in the outer layer increases with stratification. Part (c) shows the polar angle, Θ made by the wavenumber vector and the horizontal plane, based on the linear dispersion relation using the dominant frequency of $\partial w'/\partial z$. Since the calculation of Θ assumes that the internal waves are linear, it will be accurate only where the flow consists of small amplitude waves, which is generally true here for $z/\delta > 1$. Since they are generated by a three-dimensional turbulent flow, it is remarkable that the internal waves with the largest $\partial w'/\partial z$ are associated with a definite structure, namely azimuthal and polar angles approximately $35 - 60^o$ under both stratifications considered here.

It is desirable to determine the relative importance of the radiated internal waves to the energetics of the turbulent boundary layer. We can assess this by comparing the size of the terms in the turbulent kinetic energy budget. At steady state, the turbulent kinetic energy budget integrated to a height z outside the boundary layer is:

$$\int_0^z P dz' - \int_0^z \epsilon dz' - \langle p'w' \rangle - Ri_* \int_0^z \langle w'\rho' \rangle dz' = 0, \tag{2}$$

where P and ϵ are the production and dissipation, respectively, and it has been assumed that z is sufficiently large so that the turbulent transport and the viscous diffusion are negligible. Here $< \cdot >$ denotes an average over a horizontal plane and time, during a period when the fluctuations are quasi-steady. Figure 3(a) shows that the third term in Eq. (2), the vertical energy flux, is on the order of 1% of the integrated dissipation. Therefore, the energy radiated away from the boundary layer

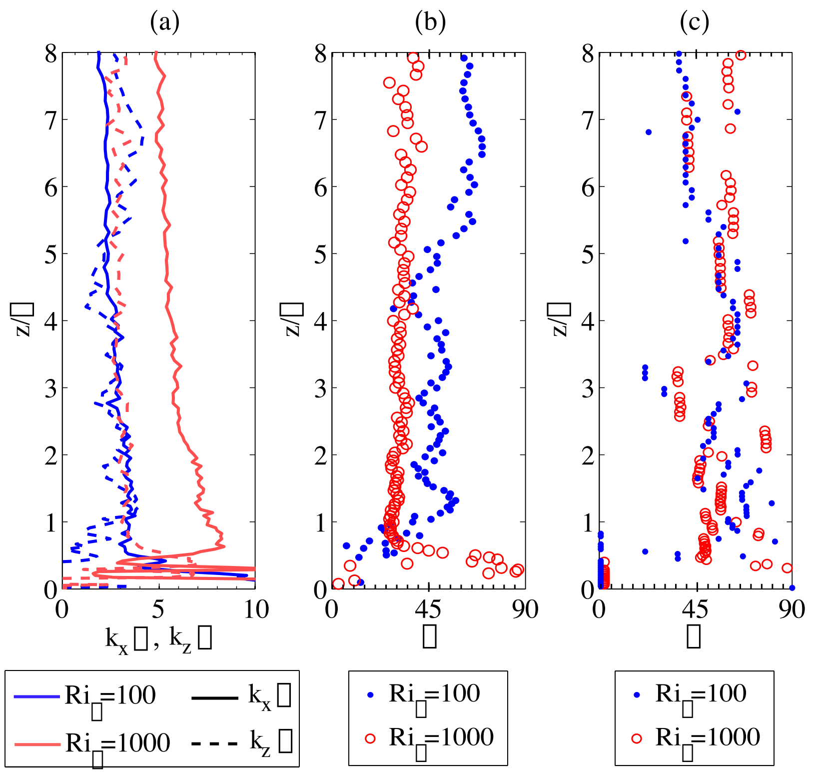

Figure 2. Characteristics of waves with the largest amplitude of $\partial w'/\partial z$. Here ϕ is the azimuthal angle and Θ is the polar angle.

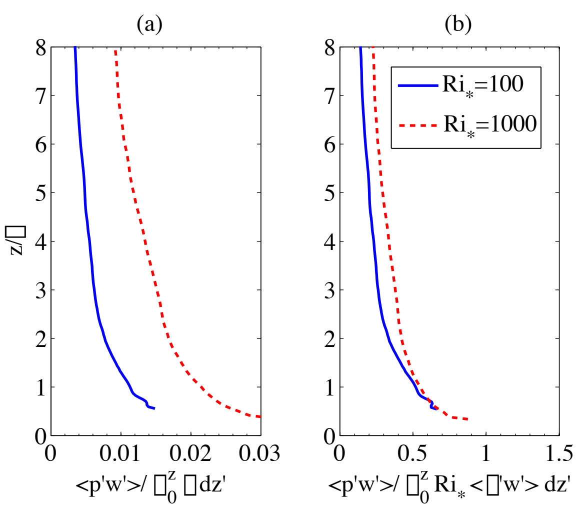

Figure 3. Vertical energy flux normalized by (a) the integrated dissipation, and (b) the integrated buoyancy flux. In order to ensure that assumptions made to derive Eq. (2) hold, the first height shown is at the top of the pycnocline where $d\langle\rho\rangle/dz = d\rho/dz_\infty$.

in the form of internal waves is negligible compared to the total energy extracted from the mean flow.

While the energy flux associated with radiated waves may be small compared to the integrated turbulent dissipation, the waves may still extract enough energy from the boundary layer to affect the evolution of the background potential energy. Since the kinetic energy is transferred to potential energy through the buoyancy flux,

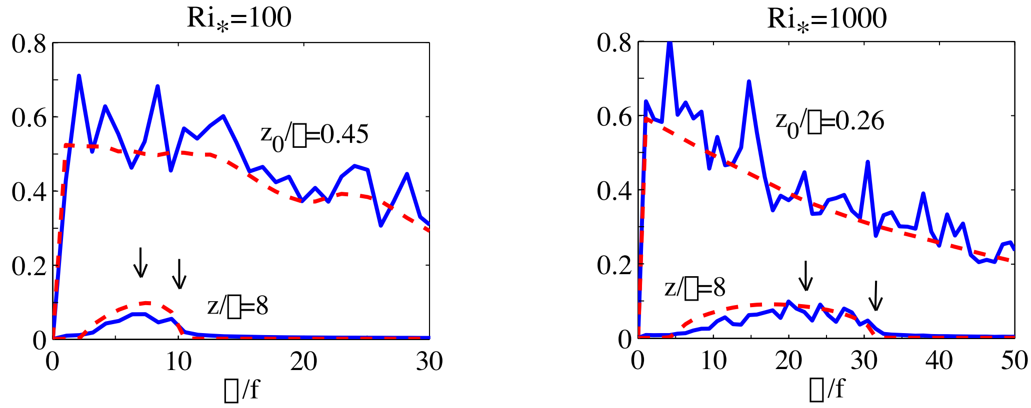

Figure 4. Comparison between observed (solid line) and predicted (dashed line) spectra of $\partial w'/\partial z$ using a viscous internal wave model. The observed wave amplitude spectra at z_0 is smoothed and then used in the internal wave model to predict the spectra at $z = 8\delta$. Arrows show $N_\infty/(\sqrt{2}f)$ (left) and N_∞/f (right).

it is useful to compare the internal wave energy flux to the integrated buoyancy flux as shown in Figure 3(b). In both cases, the outgoing energy flux at the top of the boundary layer is of the same order and the same sign as the buoyancy flux. The integrated turbulent kinetic energy budget therefore consists of the production term balanced to within a few percent by the dissipation. The rest of the energy extracted from the mean flow is either radiated away from the boundary layer by internal waves, or is transferred to mean potential energy.

4. Viscous Internal Wave Model

Although the generation of internal waves occurs in a region where nonlinear effects are important, the selection of a dominant range of frequencies for the internal waves propagating in the outer region can be explained by a simple, linear model. It is expected that the viscous damping of internal waves should depend on the wavenumber with small scale waves decaying more rapidly. In addition, waves with high and low frequencies are associated with a small vertical group velocity. Since they take longer to travel a given distance, they are therefore more susceptible to viscous decay. Starting with a known wave amplitude A_0 as a function of frequency and wavenumber at some initial location z_0, the wave amplitude at an arbitrary height $A(z)$ can be predicted based on the expected vertical propagation speed and viscous decay rate. Taylor and Sarkar [14] have shown the expected vertical velocity amplitude for linear internal waves is:

$$A(z) = A_0 \frac{|\mathbf{k}_0|}{|\mathbf{k}|} \; exp\left[\frac{-\nu\omega}{k_h}(\omega^2 - f^2)^{-1/2} \int_{z_0}^{z} |\mathbf{k}|^4 (N^2 - \omega^2)^{-1/2} dz'\right]. \qquad (3)$$

In applying this equation, it is assumed that k_h and ω remain constant for a given wave packet, while $m(z)$ is estimated from the dispersion relation. It is found that the predicted wave amplitude owing to viscous decay, found by starting with the observed amplitude A_0 at a height z_0 at the top of the mixed layer and integrating Eq. (3), compares well with the simulation as shown in Figure 4. This suggests that the frequency selection observed in Figures 1 and 2 is the result of a differential viscous decay rate.

5. Conclusions

We have conducted simulations of a turbulent Ekman layer over a flat wall. A uniform stratification was applied initially and maintained as the upper boundary condition, and the temperature gradient was set to zero at the lower wall. As the flow developed, a well-mixed, turbulent region formed near the wall, capped by a strongly stratified pycnocline. It has been established that turbulence in a bottom

Ekman layer, when subject to an overlying stratification, radiates internal waves. Considering that they were excited from a turbulent region with a broad range of frequencies and scales, it is remarkable that the turbulence-generated internal waves are associated with a distinct peak in frequency and wavenumber space. The vertical angle of propagation of these waves is between $35 - 60^o$, which is consistent with several previous studies of turbulence-generated internal waves. We have found that the vertical angle of propagation can be predicted starting with the observed wave amplitudes at the top of the mixed layer and using a linear viscous decay model.

The importance of the internal wave energy flux to the boundary layer energetics has been estimated by comparing the magnitudes of the terms in the vertically integrated turbulent kinetic energy equation. It was found that the dominant balance is between production and dissipation in the boundary layer and that the vertical energy flux is only a few percent of these terms. However, most of the production and dissipation occurs in the mixed region where stratification effects are not directly felt. We have found that the internal wave energy flux and the integrated buoyancy flux are the same order in the pycnocline. Since the buoyancy flux is a measure of the energy transferred from kinetic to potential, if all of the energy radiated away from the boundary layer as internal waves were instead present as an additional buoyancy flux, the evolution of the local mean temperature profile in the pycnocline would be significantly affected.

Acknowledgments

The support of grant N00014-05-1-0334 from ONR Physical Oceanography, program manager Dr. Scott Harper, is gratefully acknowledged.

References

[1] D.A. Aguilar and B.R. Sutherland. Internal wave generation from rough topography. *Physics of Fluids*, 18(066603):1–9, 2006.

[2] S. Basak and S. Sarkar. Dynamics of a stratified shear layer with horizontal shear. *J. Fluid Mech.*, 568:19–54, 2006.

[3] P. Bonneton, J.M. Chomaz, and E.J. Hopfinger. Internal waves produced by the turbulent wake of a sphere moving horizontally in a stratified fluid. *J. Fluid Mech.*, 254:23–40, 1993.

[4] P.J. Diamessis, J.A. Domaradzki, and J.S. Hesthaven. A spectral multidomain penalty method model for the simulation of high Reynolds number localized incompressible stratified turbulence. *Journal of Computational Physics*, 202(1):298–322, 2005.

[5] K. Dohan and B.R. Sutherland. Internal waves generated from a turbulent mixed region. *Physics of Fluids*, 15(2):488–498, 2003.

[6] K. Dohan and B.R. Sutherland. Numerical and laboratory generation of internal waves from turbulence. *Dynamics of Atmospheres and Oceans*, 40:43–56, 2005.

[7] X. E and E.J. Hopfinger. On mixing across an interface in stably stratified fluid. *J. Fluid Mech.*, 166:227–244, 1986.

[8] M.R. Flynn and B.R. Sutherland. Intrusive gravity currents and internal gravity wave generation in stratified fluid. *J. Fluid Mech.*, 514:355–383, 2004.

[9] M.J. Gourlay, S.C. Arendt, D.C. Fritts, and J. Werne. Numerical modeling of initially turbulent wakes with net momentum. *Physics of Fluids*, 13(12):3783–3802, 2001.

[10] P.F. Linden. The deepening of a mixed layer in a stratified fluid. *J. Fluid Mech.*, 71:385–405, 1975.

[11] G.R. Spedding. Vertical structure in stratified wakes with high initial Froude number. *J. Fluid Mech.*, 454:71–112, 2002.

[12] B.R. Sutherland, C.P. Caulfield, and W.R. Peltier. Internal gravity wave generation and hydrodynamic instability. *J. Atmos. Sci.*, 51(22):3261–3280, 1994.

[13] B.R. Sutherland and P.F. Linden. Internal wave excitation from stratified flow over a thin barrier. *J. Fluid Mech.*, 377:223–252, 1998.

[14] J.R. Taylor and S. Sarkar. Internal gravity waves generated by a turbulent bottom ekman layer. *J. Fluid Mech.*, in press.